



Year: 2020

Histological characterization of aldosterone-producing adrenocortical adenomas with different somatic mutations

Ono, Yoshikiyo ; Yamazaki, Yuto ; Omata, Kei ; Else, Tobias ; Tomlins, Scott A ; Rhayem, Yara ; Williams, Tracy Ann ; Reincke, Martin ; Carling, Tobias ; Monticone, Silvia ; Mulatero, Paolo ; Beuschlein, Felix ; Ito, Sadayoshi ; Satoh, Fumitoshi ; Rainey, William E ; Sasano, Hironobu

Abstract: CONTEXT Aldosterone-producing adrenocortical adenomas (APAs) are mainly composed of clear (lipid rich) and compact (eosinophilic) tumor cells. The detailed association between these histological features and somatic mutations (KCNJ5, ATP1A1, ATP2B3 and CACNA1D) in APAs is unknown. **OBJECTIVE** To examine the association between histological features and individual genotypes in APAs. **METHODS** Examination of 39 APAs subjected to targeted next-generation sequencing (11 KCNJ5, 10 ATP1A1, 10 ATP2B3, and 8 CACNA1D) and quantitative morphological and immunohistochemical (CYP11B2 and CYP17A1) analyses using digital imaging software. **RESULTS** KCNJ5- and ATP2B3-mutated APAs had clear cell dominant features [KCNJ5: clear 59.8% (54.4%-64.6 %) vs. compact 40.2% (35.4%-45.6 %), $P=0.0022$; ATP2B3: clear 54.3% (48.2%-62.4 %) vs. compact 45.7% (37.6%-51.8 %), $P=0.0696$]. ATP1A1- and CACNA1D-mutated APAs presented with marked intratumoral heterogeneity. A significantly positive correlation of immunoreactivity was detected between CYP11B2 and CYP17A1 in tumor cells of KCNJ5-mutated APAs ($P=0.0112$; $r=0.7237$), in contrast, significantly inverse correlation was detected in ATP1A1-mutated APAs ($P=0.0025$; $r=-0.8667$). **CONCLUSION** KCNJ5-mutated APAs, co-expressing CYP11B2 and CYP17A1, were more deviated in terms of zonation-specific differentiation of adrenocortical cells compared with ATP1A1- and ATP2B3- mutated APAs.

DOI: <https://doi.org/10.1210/clinem/dgz235>

Posted at the Zurich Open Repository and Archive, University of Zurich

ZORA URL: <https://doi.org/10.5167/uzh-179599>

Journal Article

Accepted Version

Originally published at:

Ono, Yoshikiyo; Yamazaki, Yuto; Omata, Kei; Else, Tobias; Tomlins, Scott A; Rhayem, Yara; Williams, Tracy Ann; Reincke, Martin; Carling, Tobias; Monticone, Silvia; Mulatero, Paolo; Beuschlein, Felix; Ito, Sadayoshi; Satoh, Fumitoshi; Rainey, William E; Sasano, Hironobu (2020). Histological characterization of aldosterone-producing adrenocortical adenomas with different somatic mutations. *Journal of Clinical Endocrinology Metabolism*, 105(3):dgz235.

DOI: <https://doi.org/10.1210/clinem/dgz235>

Histological characterization of aldosterone-producing adrenocortical adenomas with different somatic mutations

Yoshikiyo Ono^{1, 2, 3, 4}, Yuto Yamazaki², Kei Omata^{1, 2, 5, 6}, Tobias Else⁴,
Scott A. Tomlins^{5, 6, 7, 8}, Yara Rhayem⁹, Tracy Ann Williams^{9, 10}, Martin Reincke⁹,
Tobias Carling¹¹, Silvia Monticone¹⁰, Paolo Mulatero¹⁰, Felix Beuschlein^{9, 12},
Sadayoshi Ito¹, Fumitoshi Satoh^{1, 13}, William E. Rainey³, and Hironobu Sasano²

- 1) Division of Nephrology, Endocrinology, and Vascular Medicine, Tohoku University Hospital, Sendai, Japan.
- 2) Department of Pathology, Tohoku University Graduate School of Medicine, Sendai, Japan.
- 3) Departments of Molecular and Integrative Physiology & Internal Medicine, University of Michigan Medical School, Ann Arbor, MI, USA.
- 4) Division of Metabolism, Endocrine, and Diabetes, Department of Internal Medicine, University of Michigan Medical School, Ann Arbor, MI, USA
- 5) Department of Pathology, University of Michigan Medical School, Ann Arbor, MI, USA
- 6) Michigan Center for Translational Pathology, University of Michigan Medical School, Ann Arbor, MI, USA.
- 7) Department of Urology, University of Michigan Medical School, Ann Arbor, MI, USA
- 8) Comprehensive Cancer Center, University of Michigan Medical School, Ann Arbor, MI, USA.
- 9) Medizinische Klinik und Poliklinik IV, Klinikum der Universität, Ludwig-Maximilians-Universität München, Munich, Germany.
- 10) Division of Internal Medicine and Hypertension, Department of Medical Sciences, University of Torino, Torino, Italy.
- 11) Yale Endocrine Neoplasia Laboratory, Yale School of Medicine, New Haven, CT, USA.
- 12) Klinik für Endokrinologie, Diabetologie und Klinische Ernährung, Universitätsspital Zürich, Zurich, Switzerland.
- 13) Division of Clinical Hypertension, Endocrinology and Metabolism, Tohoku University Graduate School of Medicine, Sendai, Japan.

Key terms: primary aldosteronism, CYP11B2, *ATP1A1*, *ATP2B3*, *CACNA1D*, *KCNJ5*

Address for correspondence and reprint requests to :

© Endocrine Society 2019. All rights reserved. For permissions, please e-mail: journals.permissions@oup.com. jc.2019-40189. See endocrine.org/publications for Accepted Manuscript disclaimer and additional information.

Hironobu Sasano, MD, PhD

Department of Pathology, Tohoku University School of Medicine

2-1 Seiryō-machi, Aoba-ku, Sendai 980- 8575 JAPAN

Tel: +81-22-717-8050

Fax: +81-22-717-8051

E-mail: hsasano@patholo2.med.tohoku.ac.jp

Accepted Manuscript

Abstract

Context: Aldosterone-producing adrenocortical adenomas (APAs) are mainly composed of clear (lipid rich) and compact (eosinophilic) tumor cells. The detailed association between these histological features and somatic mutations (*KCNJ5*, *ATP1A1*, *ATP2B3* and *CACNA1D*) in APAs is unknown.

Objective: To examine the association between histological features and individual genotypes in APAs.

Methods: Examination of 39 APAs subjected to targeted next-generation sequencing (11 *KCNJ5*, 10 *ATP1A1*, 10 *ATP2B3*, and 8 *CACNA1D*) and quantitative morphological and immunohistochemical (CYP11B2 and CYP17A1) analyses using digital imaging software.

Results: *KCNJ5*- and *ATP2B3*-mutated APAs had clear cell dominant features [*KCNJ5*: clear 59.8% (54.4%–64.6 %) vs. compact 40.2% (35.4%–45.6 %), $P=0.0022$; *ATP2B3*: clear 54.3% (48.2%–62.4 %) vs. compact 45.7% (37.6%–51.8 %), $P=0.0696$]. *ATP1A1*- and *CACNA1D*-mutated APAs presented with marked intratumoral heterogeneity. A significantly positive correlation of immunoreactivity was detected between CYP11B2 and CYP17A1 in tumor cells of *KCNJ5*-mutated APAs ($P=0.0112$; $\rho=0.7237$), in contrast, significantly inverse correlation was detected in *ATP1A1*-mutated APAs ($P=0.0025$; $\rho=-0.8667$).

Conclusion: *KCNJ5*-mutated APAs, co-expressing CYP11B2 and CYP17A1, were more deviated in terms of zonation-specific differentiation of adrenocortical cells compared with *ATP1A1*- and *ATP2B3*- mutated APAs.

Introduction

Primary aldosteronism (PA) is one of the most common forms of secondary hypertension, accounting for approximately 10% of all hypertensive patients (1-6). Aldosterone-producing adenoma (APA) and idiopathic hyperaldosteronism (IHA) are the two major subtypes of PA (1-7). In addition, APAs are well known to harbor marked intratumoral heterogeneity in terms of their morphology, genetics and steroidogenesis (8-10). Histologically, APAs are mainly composed of two distinctive cell types based on their morphological features: “clear cells” and “compact cells” (8, 9). Clear cells are termed as “lipid-rich cells” or “zona fasciculata (ZF)-like cells” harboring relatively abundant lipid droplets, while “compact cells”, also termed as “lipid-poor cells” or “zona glomerulosa (ZG)-like cells”, are small, spherical shaped cells with eosinophilic cytoplasm (8, 9). However, an association between the morphological and functional features of these tumor cells has remained virtually unknown.

In addition, recent studies using next-generation sequencing (NGS) revealed that the great majority of APAs harbored somatic mutations of genes encoding ion channels and ion transporters (*KCNJ5* encoding the inwardly rectifying potassium channel subfamily J, member 5; *ATP1A1*, Na⁺/K⁺ ATPase 1; *ATP2B3*, Ca²⁺-ATPase 3 and *CACNA1D*, voltage-dependent, L-type calcium channel subunit 1D) (11-16). These somatic mutations were detected in approximately 90% of all APAs (14, 16, 17). Among them, somatic APA mutations in *KCNJ5* were the most frequently detected in Caucasian as well as Asian patients (11-16) whereas APA mutations in *CACNA1D* were most frequently detected in Afro-American patients (17).

Possible genotype-phenotype associations, including histological features of APAs, have been proposed especially in APAs carrying *KCNJ5* mutations (9, 18, 19). *KCNJ5*-mutated APAs have a clear cell-dominant histology and a relatively large size. In addition, Monticone et al. reported that CYP11B2 immunoreactivity was significantly more abundant in ZG-like (n=43) than in ZF-like (n=28) APAs and that *KCNJ5* somatic mutations were more frequently detected in the latter type (19). However, detailed histological features of *KCNJ5*-mutated APAs and APAs with the less frequently detected somatic mutations (*ATP1A1*, *ATP2B3* and *CACNA1D*) are unknown. In addition, the majority of histological studies cited above were performed with manual analyses, which could be associated with marked inter- and intra-observer variance (10, 15, 19). We previously proposed that a quantitative histological analytical approach using digital imaging software could minimize such variance because of high reproducibility in the analysis of *KCNJ5*-mutated APAs (9).

Therefore, in this study, we quantitatively analyzed the morphological features and immunoreactivity of CYP11B2 and CYP17A1 in combination with targeted NGS for APA genotyping. Our objective was to apply state-of-the art and quantifiable technology to establish the correlations of histologic features with the distribution of steroidogenic enzymes stratified by genotype.

Materials & Methods

APA cases

We initially retrieved the cases demonstrating *KCNJ5* wild type by initial sequencing after screening in 51 cases from all of the participating institutions (University of Michigan, Ludwig Maximilian University of Munich, University of Torino and Yale University) because of the relatively small number of the cases harboring rare frequent mutations. Subsequent further sequencing by NGS

validated the genotypes of those cases (*KCNJ5*: 11 cases, *ATP1A1*: 14 cases, *ATP2B3*: 11 cases, *CACNA1D*: 15 cases). We then exclusively analyzed the 10% formalin fixed and paraffin embedded tissue specimens prepared in the good manner without any artifacts examined by histological evaluation in hematoxylin and eosin stained tissue slides. We then selected those containing the whole area of the tumor at maximum diameter by subsequent histological examination. The screening above yielded the number of the cases examined in this study as follows (*KCNJ5*: 11 cases, *ATP1A1*: 10 cases, *ATP2B3*: 10 cases, *CACNA1D*: 8 cases).

All the cases examined were clinically diagnosed according to the Endocrine Society Guidelines for PA (1). The clinicopathological variables of these cases were summarized in Table 1. All tumors were pathologically diagnosed as adrenocortical adenomas according to the criteria of Weiss (20). Immunostaining with CYP11B2 antibody was subsequently performed to confirm the histopathological diagnosis of APAs (9, 21). We first screened all available tissue sections (average 4-5 sections) of all the cases examined and did select the representative tissue section containing the largest area of the tumor. The whole tumor areas with maximum dimension, which could reflect intratumoral heterogeneity (Fig. 1) were selected among all the available tissue sections of individual cases. This study protocol was approved by the Institutional Review Board of each institution.

Quantitative morphological analysis using digital imaging analysis (DIA)

Hematoxylin and eosin (H&E) staining was performed as reported previously (9). All H&E stained sections were digitally scanned and captured using Image Scope AT2 (Leica, Wetzlar, Germany). Digital imaging analysis (DIA) was subsequently performed using the software of HALO Area Quantification ver. 1.0 (Indica Laboratories, Corrales, NM) to minimize inter-observer variance and achieve high reproducibility as reported previously (9). In brief, the whole tumor area was first classified into tumor cell and stromal areas based on architectural patterns. We classified tumor cell areas into nuclear and cytoplasm areas based on their color spectrums, and cytoplasm areas within a tumor cell area further subclassified into clear and compact cells based on the gradients of the eosinophilic color spectrum. Two observers analyzed histological parameters in an independent manner (Y.O and Y.Y).

The ratio of each histological component against the whole tumor area was then calculated. The percentage of clear and compact cell components within the tumor cell area was also calculated.

Quantitative analysis of CYP11B2 and CYP17A1 immunoreactivity using DIA

IHC analysis was performed using the antibodies against CYP11B2 (mouse monoclonal) (22) and CYP17A1 (rabbit polyclonal) (23) as reported previously (24). All IHC sections were scanned and captured as above (9). The modified H-score system was adopted in this study to evaluate immunoreactivity of CYP11B2 and CYP17A1 in the quantitative fashion (9, 22, 24). The gradient of relative immunointensity was tentatively defined as follows: negative as “0”, weak as “+1”, moderate as “+2”, and marked as “+3”. Threshold of score 1+ and 3+ were determined based on the gradient of the color spectrum in individual cases and the threshold of score 2+ was set as the midpoint between score 1+ and 3+. H-score of the unit area (mm²) was calculated as follows: Σ (Area of the individual gradients in positive cells x Score 1+, 2+ and 3+) / tumor area [the “cytoplasm”area] (9, 22, 24, 25).

Somatic mutation analysis in APAs by next-generation sequencing

Surgically resected PA adrenals were fixed in 10% neutral-buffered formalin and paraffin embedded (formalin fixed paraffin embedded, FFPE) to prepare 5µm serial sections. Tissue samples were isolated from six unstained sections by dissecting areas corresponding to serial sections of CYP11B2 IHC as previously reported (9, 10, 21, 26, 27). Genomic DNA was extracted using AllPrep DNA/RNA FFPE kit (QIAGEN) as previously reported. (10, 21, 26, 27). In each case, 20ng of isolated gDNA was used to generate a barcoded library by multiplexed PCR using a custom Ion AmpliSeq Panel and the Ion AmpliSeq Library kit 2.0 (Life Technologies) according to the manufacturer's instructions. The custom Ion AmpliSeq Panel was designed to target the genes previously reported to be mutated in APA or other adrenal diseases (APA_v2 Panel). The APA_v2 Panel includes 499 independent primer pairs targeting the entire coding regions of genes reported to be somatically mutated in APAs (*KCNJ5*, *ATP1A1*, *ATP2B3* and *CACNA1D*). Template preparation and sequencing of multiplexed templates were performed as previously reported (10, 21, 26, 27) using Ion PI Chip on the Ion Torrent Proton sequencer (Life Technologies, Carlsbad, CA).

Statistical analysis

Multi-comparison analyses were performed for the comparison of histological factors among all genotypes of APAs examined (*KCNJ5*, *ATP1A1*, *ATP2B3* and *CACNA1D*) using Kruskal-Wallis test. The correlation between the proportion of the area of tumor cell subtypes and H-SCORE of CYP11B2 and CYP17A1 was evaluated using Spearman's correlation coefficient. P value of <0.05 was considered significant in this study. The software of JMP Pro ver.14.2.0 was used for statistical analysis.

Results

Comparison of histological features among APAs with different somatic mutations

The proportions of tumor and stromal areas were not significantly different among APAs with different genotypes. The proportion of the nuclear area in *ATP1A1*-mutated APAs was significantly higher than that in *ATP2B3*-mutated APAs [*ATP1A1*-mutated: 13.3% (9.3%–16.8 %) vs. *ATP2B3*-mutated: 8.8% (6.1%–11.1 %), $P=0.0376$]. *CACNA1D*-mutated APAs had a significantly higher nuclear/cytoplasm ratio than *ATP2B3*-mutated APAs [0.20 (0.17–0.26) vs. 0.13 (0.09–0.16), $P=0.0295$] although the proportion of cytoplasm area was not significantly different among the different genotypes examined (Table 1, Fig. 2). The proportion of the clear tumor cell component was significantly higher than that of the compact one in *KCNJ5*-mutated APAs [59.8% (54.4%–64.6 %) vs. 40.2% (35.4%–45.6%), $P=0.0022$] but not significantly higher in *ATP2B3*-mutated APAs [54.3% (48.2%–62.4%) vs. 45.7% (37.6%–51.8%), $P=0.0696$] (Table 1, Fig. 3). Both *ATP1A1*- and *CACNA1D*-mutated APAs harbored more marked histological intratumoral heterogeneity in terms of clear and compact tumor cell distribution, but there was no significant correlation between the proportion of clear or compact tumor cells and specific genotypes of APAs.

Comparison of CYP11B2 and CYP17A1 immunoreactivity among APAs with different somatic mutations

The status of CYP11B2 immunoreactivity (CYP11B2 H score/mm²) was not significantly different among *ATP1A1*-, *ATP2B3*-, *CACNA1D*- and *KCNJ5*-mutated APAs [*ATP1A1*: 0.53(0.13–0.78), *ATP2B3*: 0.57 (0.41-0.75), *CACNA1D*: 0.56 (0.10-0.97) and *KCNJ5*-mutated APA: 0.46 (0.29–0.58)]. However, CYP17A1 immunoreactivity (CYP17A1 H score/mm²) was significantly higher in *KCNJ5*-than in *ATP2B3*-mutated APAs [0.34 (0.26-0.38) vs. 0.13 (0.02-0.22), *P*=0.0057] and in *CACNA1D*-than in *ATP2B3*-mutated APAs [0.39 (0.23-0.54) vs. 0.13 (0.02-0.22), *P*=0.0184] (Table 1, Fig. 3).

Correlation between histological features and immunoreactivity of CYP11B2 and CYP17A1 in individual genotypes of APAs

In *KCNJ5*-mutated APAs, the status of CYP11B2 immunoreactivity (CYP11B2 H score/mm²) was significantly inversely correlated with the proportion of the clear tumor cell component (*P*=0.00289; ρ =−0.6545) but positively with that of compact cells (*P*=0.00289; ρ =0.6545). There were, however, no significant correlations between CYP11B2 immunoreactivity and clear/compact tumor cell component in *ATP1A1*-, *ATP2B3*- and *CACNA1D*-mutated APAs as well as between the proportion of clear/compact tumor cell component and the status of CYP17A1 immunoreactivity (CYP17A1 H score/mm²) in APAs, regardless of their somatic mutations. Of particular interest, CYP11B2 and CYP17A1 were significantly positively correlated in *KCNJ5*-mutated APAs (*P*=0.0112; ρ =0.7237) but inversely in *ATP1A1*-mutated APAs (*P*=0.0025; ρ =−0.8667). However, there were no significant correlations between CYP11B2 and CYP17A1 immunoreactivity in both *ATP2B3*- and *CACNA1D*-mutated APAs (Fig. 4).

Discussion

This is the first study demonstrating detailed quantitative morphological characteristics of APAs with different somatic mutations identified by targeted next-generation sequencing and including the relatively rare *ATP1A1*, *ATP2B3* and *CACNA1D* somatic mutations.

Histological differentiation between clear and compact tumor cells can be occasionally difficult in APAs (9). In addition, the previously proposed histological classification of APAs as “ZG” or “ZF” did not sufficiently represent the biological or functional features of tumor cells (9). Therefore, in this study, we focused on the histological characterization of tumor cells in APAs including those with relatively rare somatic mutations (*ATP1A1*, *ATP2B3* and *CACNA1D*) based on their morphological and biological or functional features.

The results of our present study revealed that clear tumor cells were indeed predominant in *KCNJ5*-mutated APAs but not in *ATP1A1*-, *ATP2B3*- and *CACNA1D*-mutated APAs, all of which demonstrated marked intratumoral morphological heterogeneity. These findings were consistent with previously reported manual analyses. (16, 19, 28-31). *ATP2B3*-mutated APAs had relatively smaller nuclei than *ATP1A1*-mutated APAs and lower nuclear to cytoplasm ratios than *CACNA1D*-mutated APAs, indicating that *ATP2B3*-mutated APAs had smaller nuclei but relatively more abundant cytoplasm containing lipid droplets than APAs with other genotypes. Thus, it has become important to explore the functional significance of these histological differences among different mutated APAs.

The status of CYP11B2 immunoreactivity was not significantly different among *KCNJ5*-, *ATP1A1*-, *ATP2B3*- and *CACNA1D*-mutated APAs. These findings did indicate that there were no significant differences concerning intratumoral aldosterone biosynthesis among APAs with different somatic mutations. However, the status of CYP17A1 immunoreactivity in tumor cells was indeed significantly lower in *ATP2B3*-mutated APAs than in *CACNA1D*- and *KCNJ5*-mutated APAs. These findings all demonstrated that *ATP2B3*-mutated APAs could have relatively lower capability of neoplastic aberrant cortisol and aldosterone biosynthesis compared to *KCNJ5*- and *CACNA1D*-mutated APAs. However, further studies including the analysis of co-secretion of cortisol or other glucocorticoids possibly demonstrated by the dexamethasone suppression test and of secretion of hybrid steroids such as 18-oxocortisol in order to explore the biological significance of the findings above.

KCNJ5-mutated APAs are larger and more abundant clear cell dominant tumors with a much higher frequency of neoplastic aldosterone and cortisol co-secretion than non-*KCNJ5*-mutated genotypes (32-34). In this study, both CYP11B2 and CYP17A in tumor cells of *KCNJ5*-mutated APAs were significantly more abundant than in those of APAs of other genotypes. Hybrid tumor cells which co-expressed CYP11B1+/CYP11B2+ and/or CYP17A+/CYP11B2+, and even triple positive hybrid cells (CYP17A+/CYP11B1+/CYP11B2+) have been reported in APAs (33, 34). These hybrid cells were also reported to be specific for APAs, as they were not detected in normal or hyperplastic aldosterone producing cortical cells (31, 33). Tezuka et al., also recently reported that these hybrid cells were significantly more abundant and synthesized increased amounts of hybrid steroids such as 18-oxocortisol in *KCNJ5*-mutated APAs compared with non *KCNJ5*-mutated APAs (34). These finding also indicated that *KCNJ5*-mutated APAs could represent more deviated features from zonation-based differentiation of normal adrenocortical cells.

ATP2B3-mutated APAs demonstrated relative clear cell dominant histology but CYP11B2 and CYP17A in tumor cells did not necessarily show a positive correlation. *ATP1A1*-mutated APAs had more compact or eosinophilic tumor cells than other genotypes despite a more pronounced intratumoral morphological heterogeneity. Of particular interest, CYP11B2 and CYP17A in tumor cells showed an inverse correlation in *ATP1A1*-mutated APAs. These findings all indicated that *ATP1A1*- and *ATP2B3*-mutated APAs displayed a more zonation-based or organized differentiation than *KCNJ5*-mutated APAs. In addition, aldosterone biosynthesis in these tumors was more similar to that in normal or hyperplastic zona glomerulosa. There were no significant correlations in *CACNA1D*-mutated APAs in contrast to *KCNJ5*-, *ATP1A1*- and *ATP2B3*-mutated APAs. Therefore, further investigations are required to clarify the mechanistic aspects of the correlation between individual somatic mutations and the phenotypes revealed by our present study to achieve a better understanding of neoplastic aldosterone overproduction in APAs.

Sources of Funding

M Reincke is supported by the European Research Council (ERC) under the European Union's Horizon 2020 research and innovation programme (grant agreement No [694913]), F Beuschlein, M Reincke and TA Williams are supported by the Deutsche Forschungsgemeinschaft (DFG, German Research Foundation) Projektnummer: 314061271-TRR 205. T Else is sponsored by NHLBI (5R01HL130106-04). This study was also supported by the Friedrich Baur Stiftung (F-B-S), grant number 46/16 "Genetics and Tissue-based Metabolomics of Aldosterone Producing Adenoma" awarded to Y. Rhayem. F Satoh and H Sasano have received grants from the Ministry of Health, Labour, and Welfare, Japan (No. H29-Nanji-Ippan-046).

Disclosures

The authors have nothing to disclose.

Accepted Manuscript

References

- [1] Funder JW, Carey RM, Mantero F, Murad MH, Reincke M, Shibata H, Stowasser M, Young WF Jr. The Management of Primary Aldosteronism: Case Detection, Diagnosis, and Treatment: An Endocrine Society Clinical Practice Guideline. *J Clin Endocrinol Metab*. 2016;101:1889-916.
- [2] Mulatero P, Stowasser M, Loh KC, Fardella CE, Gordon RD, Mosso L, Gomez-Sanchez CE, Veglio F, Young WF Jr. Increased diagnosis of primary aldosteronism, including surgically correctable forms, in centers from five continents. *J Clin Endocrinol Metab*. 2004;89:1045-50.
- [3] Rossi GP, Bernini G, Caliumi C, Desideri G, Fabris B, Ferri C, Ganzaroli C, Giacchetti G, Letizia C, Maccario M, Mallamaci F, Mannelli M, Mattarello MJ, Moretti A, Palumbo G, Parenti G, Porteri E, Semplicini A, Rizzoni D, Rossi E, Boscaro M, Pessina AC, Mantero F; PAPY Study Investigators. A prospective study of the prevalence of primary aldosteronism in 1,125 hypertensive patients. *J Am Coll Cardiol*. 2006;48:2293-2300.
- [4] Stowasser M, Taylor PJ, Pimenta E, Ahmed AH, Gordon RD. Laboratory investigation of primary aldosteronism. *Clin Biochem Rev*. 2010;31:39-56.
- [5] Hannemann A, Bidlingmaier M, Friedrich N, Manolopoulou J, Spyroglou A, Völzke H, Beuschlein F, Seissler J, Rettig R, Felix SB, Biffar R, Döring A, Meisinger C, Peters A, Wichmann HE, Nauck M, Wallaschofski H, Reincke M. Screening for primary aldosteronism in hypertensive subjects: results from two German epidemiological studies. *Eur J Endocrinol*. 2012;167:7-15.
- [6] Calhoun DA. Hyperaldosteronism as a common cause of resistant hypertension. *Annu Rev Med*. 2013;64:233-47.
- [7] Satoh F, Abe T, Tanemoto M, Nakamura M, Abe M, Uruno A, Morimoto R, Sato A, Takase K, Ishidoya S, Yoichi Arai, Takashi Suzuki, Hironobu Sasano, Tadashi Ishibashi. Localization of aldosterone-producing adrenocortical adenomas: significance of adrenal venous sampling. *Hypertension Res*. 2007;30:1083-95.
- [8] Neville AM, O'Hare MJ. The Human Adrenal Cortex: Pathology and Biology-An Integrated Approach. Berlin, Germany: Springer-Verlag; 1982.
- [9] Yamazaki Y, Omata K, Tezuka Y, Ono Y, Morimoto R, Adachi Y, Ise K, Nakamura Y, Gomez-Sanchez CE, Shibahara Y, Kitamoto T, Nishikawa T, Ito S, Satoh F. Tumor cell subtypes based on the intracellular hormonal activity in *KCNJ5* mutated aldosterone-producing adenoma. *Hypertension*. 2018;72:632-40.
- [10] Nanba K, Chen AX, Omata K, Vinco M, Giordano TJ, Else T, Hammer GD, Tomlins SA, Rainey WE. Molecular heterogeneity in aldosterone-producing adenomas. *J Clin Endocrinol Metab*. 2016;101:999-1007.
- [11] Choi M, Scholl UI, Yue P, Björklund P, Zhao B, Nelson-Williams C, Ji W, Cho Y, Patel A, Men CJ, Lolis E, Wisgerhof MV, Geller DS, Mane S, Hellman P, Westin G, Åkerström G, Wang W, Carling T, Lifton RP. Kt channel mutations in adrenal aldosterone producing adenomas and hereditary hypertension. *Science*. 2011;331:768-72.
- [12] Beuschlein F, Boulkroun S, Osswald A, Wieland T, Nielsen HN, Lichtenauer UD, Penton D, Schack VR, Amar L, Fischer E, Walther A, Tauber P, Schwarzmayer T, Diener S, Graf E, Allolio B,

Samson-Couterie B, Benecke A, Quinkler M, Fallo F, Plouin PF, Mantero F, Meitinger T, Mulatero P, Jeunemaitre X, Warth R, Vilsen B, Zennaro MC, Strom TM, Reincke M. Somatic mutations in *ATP1A1* and *ATP2B3* lead to aldosterone-producing adenomas and secondary hypertension. *Nat Genet.* 2013;45:440-44.

[13] Åkerström T, Maharjan R, Sven Willenberg H, Cupisti K, Ip J, Moser A, Ståhlberg P, Robinson B, Alexander Iwen K, Dralle H, Walz MK, Lehnert H, Sidhu S, Gomez-Sanchez C, Hellman P, Björklund P. Activating mutations in CTNNB1 in aldosterone producing adenomas. *Sci Rep.* 2016 Jan 27;6:19546.

[14] Berthon A, Drelon C, Ragazzon B, Boulkroun S, Tissier F, Amar L, Samson-Couterie B, Zennaro MC, Plouin PF, Skah S, Plateroti M, Lefèbvre H, Sahut-Barnola I, Batisse-Lignier M, Assié G, Lefrançois-Martinez AM, Bertherat J, Martinez A, Val P. WNT/b-catenin signaling is activated in aldosterone-producing adenomas and controls aldosterone production. *Human Molecular Genetics*, 2014;23:889–905.

[15] Scholl UI, Healy JM, Thiel A, Fonseca AL, Brown TC, Kunstman JW, Horne MJ, Dietrich D, Riemer J, Kücüköylü S, Reimer EN, Reis AC, Goh G, Kristiansen G, Mahajan A, Korah R, Lifton RP, Prasad ML, Carling T. Novel somatic mutations in primary hyperaldosteronism are related to the clinical, radiological and pathological phenotype. *Clin Endocrinol (Oxf)*. 2015;83:779-89.

[16] Fernandes-Rosa FL, Williams TA, Riester A, Steichen O, Beuschlein F, Boulkroun S, Strom TM, Monticone S, Amar L, Meatchi T, Mantero F, Cicala MV, Quinkler M, Fallo F, Allolio B, Bernini G, Maccario M, Giacchetti G, Jeunemaitre X, Mulatero P, Reincke M, Zennaro MC. Genetic spectrum and clinical correlates of somatic mutations in aldosterone-producing adenoma. *Hypertension*. 2014;64:354–61.

[17] Nanba K, Omata K, Gomez-Sanchez CE, Stratakis CA, Demidowich AP, Suzuki M, Thompson LDR, Cohen DL, Luther JM, Gellert L, Vaidya A, Barletta JA, Else T, Giordano TJ, Tomlins SA, Rainey WE. Genetic characteristics of aldosterone-producing adenomas in Blacks. *Hypertension*. 2019;73(4):885-92.

[18] Lenzini L, Rossitto G, Maiolino G, Letizia C, Funder JW, Rossi GP. A Meta-Analysis of Somatic *KCNJ5* K(+) Channel Mutations In 1636 Patients With an Aldosterone-Producing Adenoma. *J Clin Endocrinol Metab.* 2015;100:E1089-95

[19] Monticone S, Castellano I, Versace K, Lucatello B, Veglio F, Gomez-Sanchez CE, Williams TA, Mulatero P. *Mol Cell Endocrinol.* 2015;411:146-54.

[20] Weiss LM Comparative histologic study of 43 metastasizing and nonmetastasizing adrenocortical tumors. *Am J Surg Pathol.* 1984;8:163–69.

[21] Yamazaki Y, Nakamura Y, Omata K, Ise K, Tezuka Y, Ono Y, Morimoto R, Nozawa Y, Gomez-Sanchez CE, Tomlins SA, Rainey WE, Ito S, Satoh F, Sasano H. Histopathological classification of cross-sectional image negative hyperaldosteronism. *J Clin Endocrinol Metab.* 2017;102:1182–192.

[22] Gomez-Sanchez CE, Qi X, Velarde-Miranda C, Plonczynski MW, Richard Parker C, Rainey W, Satoh F, Maekawa T, Nakamura Y, Sasano H, Gomez-Sanchez EP. Development of monoclonal antibodies against human CYP11B1 and CYP11B2. *Mol Cell Endocrinol.* 2014;383:111–17.

- [23] Nakamura Y, Kurotaki Y, Ise K, Felizola SJ, McNamara KM, Sasano H. *GATA6, SF1, NGFIB* and *DAX1* in the remodeled subcapsular zones in primary aldosteronism. *Endocr J*. 2014;61:393-401.
- [24] Konosu-Fukaya S, Nakamura Y, Satoh F, Felizola S.J, Maekawa T, Ono Y, Morimoto R, Ise K, Takeda K, Katsu K, Fujishima F, Kasajima A, Watanabe M, Arai Y, Gomez-Sanchez E.P, Gomez-Sanchez C.E, Doi M, Okamura H, Sasano H. β -hydroxysteroid dehydrogenase isoforms in human aldosterone-producing adenoma. *Mol Cell Endocrinol*. 2015;408:205–12.
- [25] McCarty KS Jr., Miller LS, Cox EB, Konrath J, McCarty KS, Sr. Estrogen receptor analyses. Correlation of biochemical and immunohistochemical methods using monoclonal antireceptor antibodies. *Arch Pathol Lab Med*. 1985;109:716–21.
- [26] Omata K, Yamazaki Y, Nakamura Y, Anand SK, Barletta JA, Sasano H, Rainey WE, Tomlins SA, Vaidya A. Genetic and histopathologic intertumor heterogeneity in primary aldosteronism. *J Clin Endocrinol Metab*. 2017;102:1792-96.
- [27] Omata K, Anand SK, Hovelson DH, Liu CJ, Yamazaki Y, Nakamura Y, Ito S, Satoh F, Sasano H, Rainey WE, Tomlins SA. Aldosterone-producing cell clusters frequently harbor somatic mutations and accumulate with age in normal adrenals. *J Endocr Soc*. 2017;1:787-99.
- [28] Azizan EA, Poulsen H, Tuluc P, Zhou J, Clausen MV, Lieb A, Maniero C, Garg S, Bochukova EG, Zhao W, Shaikh LH, Brighton CA, Teo AE, Davenport AP, Dekkers T, Tops B, Küsters B, Ceral J, Yeo GS, Neogi SG, McFarlane I, Rosenfeld N, Marass F, Hadfield J, Margas W, Chaggar K, Solar M, Deinum J, Dolphin AC, Farooqi IS, Striessnig J, Nissen P, Brown MJ. Somatic mutations in *ATP1A1* and *CACNA1D* underlie a common subtype of adrenal hypertension. *Nat Genet*. 2013;45:1055–60.
- [29] Kitamoto T, Suematsu S, Yamazaki Y, Nakamura Y, Sasano H, Matsuzawa Y, Saito J, Omura M, Nishikawa T. Clinical and steroidogenic characteristics of aldosterone-producing adenomas with *ATPase* or *CACNA1D* gene mutations. *J Clin Endocrinol Metab*. 2016;101:494–503.
- [30] Scholl UI, Healy JM, Thiel A, Fonseca AL, Brown TC, Kunstman JW, Horne MJ, Dietrich D, Riemer J, Küçüköylü S, Reimer EN, Reis AC, Goh G, Kristiansen G, Mahajan A, Korah R, Lifton RP, Prasad ML, Carling T. Novel somatic mutations in primary hyperaldosteronism are related to the clinical, radiological and pathological phenotype. *Clin Endocrinol*. 2015;83:779–89.
- [31] Nakamura Y, Maekawa T, Felizola SJ, Satoh F, Qi X, Velarde-Miranda C, Plonczynski MW, Ise K, Kikuchi K, Rainey WE, Gomez-Sanchez EP, Gomez-Sanchez CE, Sasano H. Adrenal CYP11B1/2 expression in primary aldosteronism: Immunohistochemical analysis using novel monoclonal antibodies. *Mol Cell Endocrinol*. 2014;392:73-9.
- [32] Ono Y, Nakamura Y, Maekawa T, Felizola SJ, Morimoto R, Iwakura Y, Kudo M, Seiji K, Takase K, Arai Y, Gomez-Sanchez CE, Ito S, Sasano H, Satoh F. Different expression of 11β -hydroxylase and aldosterone synthase between aldosterone-producing microadenomas and macroadenomas. *Hypertension*. 2014;64:438–44.
- [33] Nakamura Y, Kitada M, Satoh F, Maekawa T, Morimoto R, Yamazaki Y, Ise K, Gomez-Sanchez CE, Ito S, Arai Y, Dezawa M, Sasano H. Intratumoral heterogeneity of steroidogenesis in aldosterone-producing adenoma revealed by intensive double- and triple-immunostaining for CYP11B2/B1 and CYP17. *Mol Cell Endocrinol*. 2016 Feb 15;422:57-63.

[34] Tezuka Y, Yamazaki Y, Kitada M, Morimoto R, Kudo M, Seiji K, Takase K, Kawasaki Y, Mitsuzuka K, Ito A, Nishikawa J, Asai N, Nakamura Y, Gomez-Sanchez CE, Ito S, Dezawa M, Sasano H, Satoh F. 18-Oxocortisol Synthesis in Aldosterone-Producing Adrenocortical Adenoma and Significance of *KCNJ5* Mutation Status. *Hypertension*. 2019 Jun;73(6):1283-90.

Figure Legends

Fig. 1. Representative microphotographs of *ATP1A1*-, *ATP2B3*-, *CACNA1D*- and *KCNJ5*-mutated APA tissue sections stained with hematoxylin and eosin (H&E), and immunostained using antibodies against CYP11B2 and CYP17A1

Fig. 2. Comparison of histological features of *ATP1A1*-, *ATP2B3*-, *CACNA1D*- and *KCNJ5*-mutated APAs (A-G). The proportion of nuclear area was significantly higher in *ATP1A1*-mutated APAs than in *ATP2B3*-mutated APAs. [*ATP1A1*: 13.3% (9.3%–16.8%) versus *ATP2B3*: 8.8% (6.1%–12.0%), $P<0.05$]. The nuclear to cytoplasm ratio was significantly higher in *CACNA1D*-mutated APAs than in *ATP2B3*-mutated APAs [0.20 (0.17–0.26) versus 0.13 (0.09–0.16); $P<0.05$].

Fig. 3. Comparison of clear and compact tumor cell ratios in *ATP1A1*-, *ATP2B3*-, *CACNA1D*- and *KCNJ5*-mutated APAs (A-D). The ratio of the clear cell component tended to be more abundant than the compact cell component in *ATP2B3*-mutated APAs [54.3% (48.2%–62.4%); versus 45.7% (37.6%–51.8%); $P=0.0696$]. In *KCNJ5*-mutated APAs, the clear cell component was significantly much higher than the compact cell component [59.8% (54.4%–64.6%) versus 40.2% (35.4%–45.6%); $P=0.0022$]. Comparison of the H-score of CYP11B2 and CYP17A1 among *ATP1A1*-, *ATP2B3*-, *CACNA1D*- and *KCNJ5*-mutated APAs (E, F). The status of CYP17A immunoreactivity was significant different between *KCNJ5* and *ATP2B3* ($P=0.0057$), as well as between *ATP2B3*- and *CACNA1D*-mutated APAs ($P=0.0184$).

Fig. 4. Correlation between histological components and steroidogenic enzymes in *ATP1A1*- (A-E), *ATP2B3*- (F-J), *CACNA1D*- (K-O) and *KCNJ5*- (P-T) mutated APAs. Correlation between CYP11B2 immunoreactivity and proportion of clear cell area (A, F, K and P). Correlation between CYP11B2 immunoreactivity and proportion of compact cell area (B, G, L and Q). Correlation between the proportion of clear cell area and CYP17A1 immunoreactivity (C, H, M and R). Correlation between the proportions of compact cell area and CYP17A1 immunoreactivity (D, I, N and S). Correlation between the immunoreactivity of CYP11B2 and CYP17A1 (E, J, O and T). E, Both CYP11B2 and CYP17A1 showed a significant inverse correlation in *ATP1A1*-mutated APAs ($P=0.0025$; $\rho=-0.8667$). P, CYP11B2 immunoreactivity also showed a significant inverse correlation with the proportion of clear cell area in *KCNJ5*-mutated APAs ($P=0.0289$; $\rho=-0.6545$). Q, CYP11B2 immunoreactivity showed a significant correlation with the proportion of compact cell area in *KCNJ5*-mutated APAs ($P=0.0289$; $\rho=0.6545$). T, Both CYP11B2 and CYP17A1 showed a significant correlation ($P=0.0112$; $\rho=0.7237$) in *KCNJ5*-mutated APAs.

Mean±SEM [25-75th percentile]	<i>ATP1A1</i>	<i>ATP2B3</i>	<i>CACNA1D</i>	<i>KCNJ5</i>
N	10	10	8	11
Gender (Male/Female)	9/1	8/2	5/3	3/8
Age at adrenalectomy (years)	50.8±2.7 [41.5-58.5]	54.9±2.6 [52.0-62.0]	47.5±2.0 [42.3-53.5]	42.2±2.8 [35.0-48.0]
Baseline systolic blood pressure (mmHg)	158.4±6.7 [140.5-172.3]	166.2±5.4 [150.0-178.0]	146.9±5.8 [135.0-154.5]	140.8±7.2 [125.0-153.0]
Baseline diastolic blood pressure (mmHg)	90.2±4.1 [84.0-97.5]	94.6±2.7 [90.0-100.0]	92.8±4.3 [85.5-100.0]	82.6±5.0 [72.0-100.0]
Maximal tumor Size (mm)	13.4±1.5 [9.0-15.3]	16.3±1.4 [14.0-19.0]	11.4±1.2 [8.3-14.5]	20.7±1.5 [15.0-24.0]
Nadir serum K ⁺ (mmol/L)	2.8±0.14 [2.5-3.2]	2.7±0.1 [2.4-3.1]	3.1±0.1 [2.6-3.5]	3.4±0.2 [2.9-3.5]
Baseline plasma aldosterone concentration (PAC) (ng/dL)	46.8±9.7 [12.4-74.1]	79.8±21.0 [27.5-162.2]	49.0±14.5 [17.4-60.6]	37.1±5.8 [24.7-47.0]
Baseline active renin concentration (ARC) (mU/L)	4.6±1.6 [1.2-9.1]	7.5±4.7 [0.8-9.0]	8.2±1.6 [5.1-12.2]	n.d.
Baseline plasma renin activity (PRA) (ng/ml/hr)	0.8±0.1 [0.6-1.0]	0.6±0.4 [0.15-1.4]	0.3±0.1 [0.1-0.5]	0.2±0.1 [0.1-0.2]
Baseline PAC/ARC ratio (ng/mU)	158.7±78.5 [40.5-175.8]	411.9±116.7 [127.0-682.0]	60.1±22.5 [16.7-114.3]	n.d.
Baseline PAC/PRA ratio (ng/dL/ng/ml/hr)	68.6±16.0 [33.4-101.6]	152.0±65.6 [40.4-285.0]	188.4±67.0 [58.4-317.5]	270.1±64.8 [133.0-333.0]
PAC post 240 min. saline infusion test (ng/dL)	26.2±10.8 [10.5-25.7]	43.1±19.8 [11.5-57.7]	22.5±4.5 [11.5-24.7]	30.8±10.8 [18.0-52.3]
Tumor cell area (%)	80.4±2.9 [71.7-89.3]	74.8±2.7 [67.2-80.1]	70.9±3.1 [60.9-77.8]	73.5±4.0 [67.9-84.4]
Stroma area (%)	19.6±2.9 [10.7-28.3]	25.2±2.7 [20.0-32.9]	29.1±3.1 [22.2-39.1]	26.5±4.0 [15.7-32.2]
Nuclear area (%)	13.3±1.7 [9.3-16.8]	8.8±0.8 [6.1-11.1]	11.6±1.4 [9.9-13.6]	10.0±1.2 [6.7-12.6]
Cytoplasm area (%)	67.2±3.8 [58.8-77.9]	66.0±2.2 [59.8-70.8]	59.3±3.0 [49.6-65.4]	63.5±3.5 [60.3-69.8]
Nuclear/Cytoplasm ratio	0.21±0.03 [0.15-0.29]	0.13±0.01 [0.09-0.16]	0.20±0.02 [0.17-0.26]	0.16±0.02 [0.11-0.21]
Clear	32.9±3.9 [23.9-45.8]	35.6±2.4 [31.0-39.2]	27.4±4.8 [17.8-38.2]	38.0±2.9 [32.8-45.2]

Compact	34.2±5.5 [21.0-40.9]	30.4±3.1 [23.1-33.7]	31.9±3.7 [26.7-40.5]	25.5±2.5 [18.5-28.8]
Clear/Cytoplasm	50.3±6.0 [39.0-67.4]	54.3±3.4 [48.2-62.4]	45.1±6.8 [30.2-58.9]	59.8±3.1 [54.4-64.6]
Compact/Cytoplasm	49.7±6.0 [32.6-61.0]	45.7±3.4 [37.6-51.8]	54.9±6.8 [41.2-69.8]	40.2±3.1 [35.4-45.6]
CYP11B2 positive area (%)	34.2±5.9 [12.9-52.6]	44.7±4.4 [39.0-55.2]	34.4±6.7 [10.4-53.9]	35.5±3.7 [25.9-47.1]
CYP11B2 H-score	0.53±0.12 [0.13-0.78]	0.57±0.08 [0.41-0.75]	0.56±0.13 [0.1-0.97]	0.46±0.06 [0.29-0.58]
CYP17A1 positive area (%)	25.4±6.6 [3.4-42.1]	11.8±4.2 [2.4-18.0]	32.5±6.0 [21.7-45.1]	32.2±3.2 [25.4-37.4]
CYP17A1 H-score	0.27±0.07 [0.04-0.43]	0.13±0.05 [0.02-0.22]	0.39±0.09 [0.23-0.54]	0.34±0.04 [0.26-0.38]

Table. Clinicopathological characteristics of aldosterone-producing adenoma (APA) cases with ATP1A1, ATP2B3, CACNA1D and KCNJ5 mutation examined in this study. Value: Mean±SEM [25-75th percentile].

Figure1_09252019_0

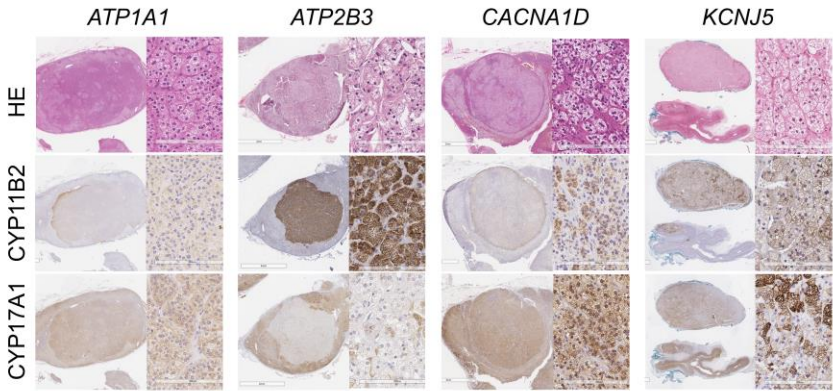


Figure2_09252019_0

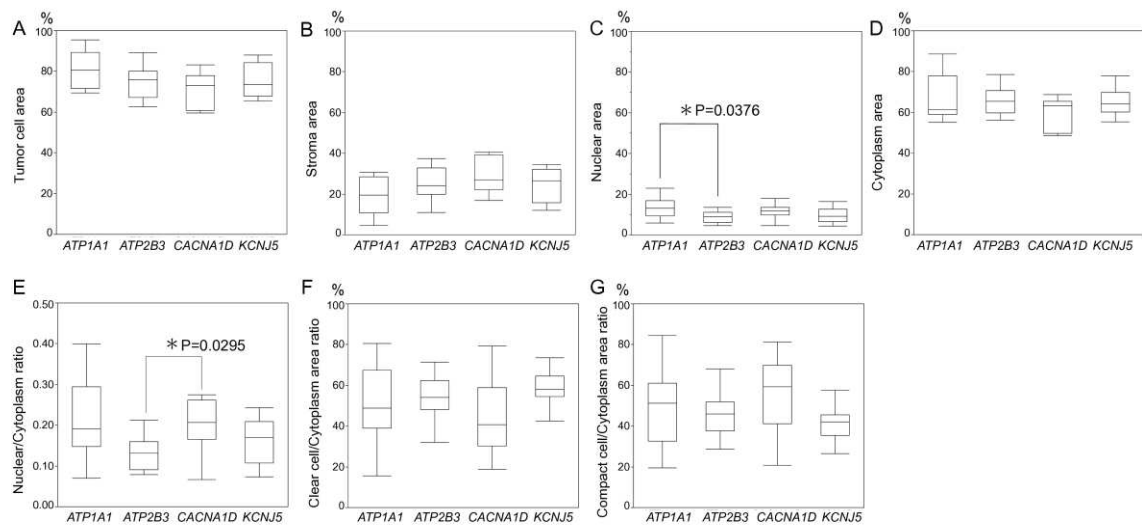


Figure3_09252019_0

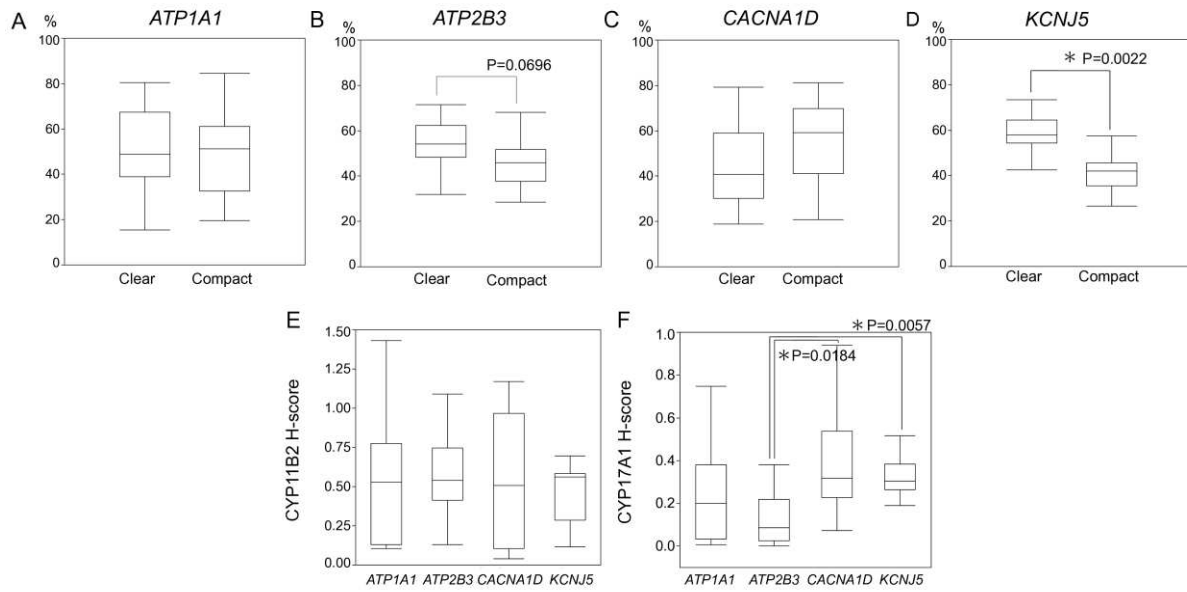


Figure4_09252019_0

